Preparation and Characterization of Asymmetric Polysulfone Membrane for Separation of Oxygen and Nitrogen Gases

S. S. Madaeni, P. Moradi

Membrane Research Center, Department of Chemical Engineering, Razi University, Kermanshah, Iran

Received 30 March 2010; accepted 16 November 2010
DOI 10.1002/app.33804
Published online 16 March 2011 in Wiley Online Library (wileyonlinelibrary.com).

ABSTRACT: Defect-free skinned asymmetric gas separation membranes were prepared by a dual bath coagulation method using a wet phase inversion technique. The membranes were cast from polysulfone solution in different solvents such as: dimethyl-formamid, 1-methyl-2-pyrrolidone, *N-N*-dimethyl-acetamide (DMAC), and tetrahydrofuran. The mixtures of water/iso-propanol (IPA), water/propanol, water/ethanol (EtOH), and water/methanol (MeOH) with volume ratio of 80/20 were used as the first coagulation bath. This led to the formation of a dense skin top layer. Distillated water was used as the second coagulation bath. The influences of several experimental variables, such as thickness of the membrane, polymer concentration, type of solvent and nonsolvent, immersion time in IPA 20%, and second coagulation bath temperature on skin layer and sublayer were elucidated. For preparing membrane with higher permeance, the influence of internal nonsolvents and addition of polyvinylpyrrolidone (PVP) as additive were investigated. The membrane performance was tested in terms of gas permeance and selectivity for O_2/N_2 separation. © 2011 Wiley Periodicals, Inc. J Appl Polym Sci 121: 2157–2167, 2011

Key words: polysulfone; defect-free asymmetric membrane; dual bath method; wet phase inversion technique

INTRODUCTION

During the past two decades membrane separation processes have been developed and optimized for large scale industrial applications. Membrane technology for separating gases is likely to play an increasingly important role in reducing the environmental impact and costs of industrial processes. Membrane separation of gases has emerged into an important unit operations technique offering advantages over conventional separation procedures.[1]

Regarding the membrane preparation, it is very difficult to make an ultrathin and defect-free top layer from a glassy polymer. However, two phase inversion process including dual[2] and evaporation[3] methods can be used to prepare a defect-free asymmetric membrane. These processes include dry, dry/wet, and wet/wet phase separation. A dry/wet phase separation process can be used to form ultrathin and defect-free asymmetric membranes using several glassy polymers.[2,4] The evaporation process is dry step requiring loss of a volatile solvent from a casting solution containing a less volatile nonsolvent component. The selective loss of the volatile solvent leads to the formation of the top skin layer of the membrane. Interfacial dry phase separation can be observed by the almost instantaneous onset of turbidity in the top skin layer region. The membrane is then immersed in a nonsolvent coagulant that is a wet-phase separation step. In this quench step, the bulk of the membrane structure is formed and the remaining solvents and nonsolvents are extracted.

In wet/wet phase separation process, membranes are formed by contacting polymer solution with two nonsolvent baths in series. The first bath is used to obtain a concentrated layer of polymer at the interface. This step makes ultrathin skin top layer similar to the evaporation step of dry/wet phase separation process. The second bath is responsible for the actual coagulation to be precipitated. The choice of nonsolvents for the bath strongly depends upon the type of solvent to be dissolved in the polymer solution. At the first bath, ultrathin layer is formed. This step is the delayed liquid–liquid phase separation process to make a dense skin layer. Although this results in a dense top layer, it usually contains defects and has no gas separation property. Therefore, this step requires a precise technique to make an ultrathin and defect-free skin top layer. The polymer concentration in the sublayer is hardly changed when the phase separation process starts. A relatively open substructure like sponge-type is formed. At the second bath, the substructure is formed as a result of

Correspondence to: S. S. Madaeni (smadaeni@yahoo.com).

the precipitation process. This is an instantaneous phase separation.

The selection of an appropriate polymeric membrane material depends on the required separation task. Most of the membrane gas separation processes are mainly focused on glassy type polymers due to superior gas selectivity and excellent thermal and mechanical properties.

Polysulfone (PSF) is widely used for gas separation due to satisfactory gas permeance and acceptable selectivity.[5] PSF is an amorphous thermoplastic polymer with glass transition temperature of 190°C. This is a flame retardant polymer, possesses high mechanical, thermal and oxidative stability[6] and is soluble in common organic solvents. Preparation of PSF membranes by phase inversion is a wel-known process.[7,8] Moreover, its relative low cost established PSF as the polymer in choice for fabrication of membranes.[5]

In this study, PSF was selected as the base material for preparation of defect-free gas separation asymmetric membrane using a wet/wet process. The effects of several variables such as membrane thickness, polymer concentration, type of solvent and nonsolvent, immersion time, coagulation bath temperature, and addition of additive to the casting solution were examined. The structures of the membranes were elucidated using scanning electron microscopy (SEM). The membrane performance was estimated for oxygen/nitrogen permeance and selectivity.

EXPERIMENTAL

Materials

PSF (average M_n 22,000 by MO beads) was supplied by Sigma–Aldrich Co. (USA). PSF resin was first dried for at least 24 h in an oven at 80°C. Figure 1 shows the chemical structure of PSF. The solvents [1-methyl-2-pyrrolidone (NMP), *N*-*N*-dimethyl-acetamide (DMAC), tetrahydrofuran (THF), $CHCl_3$, and dimethyl-formamid (DMF)] were supplied by Merck (Germany). Organic nonsolvents [BuOH, iso-propanol (IPA), propanol (PrOH), EtOH, and MeOH] were purchased from Merck (Germany). PVP with 25,000 g/mol molecular weight from Merck was used as additive. Distilled water was used for all experiments. All gases were provided in 40 L gas cylinders with 99.99% purity equipped with gas pressure regulators.

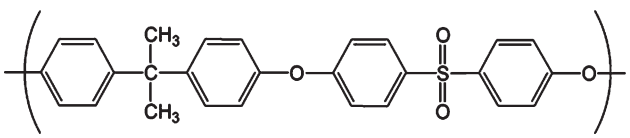

Figure 1 Chemical structure of PSF.

Membrane preparation

Asymmetric membranes were prepared by the wet phase inversion technique. The polymer solution was cast on glass plate by film applicator from PSF solution in different solvents such as DMF, NMP, DMAC, and THF. The membranes were immersed in the first coagulation bath (namely external nonsolvent) containing various alcohols immediately after casting. The mixtures of water/IPA, water/PrOH, water/ethanol (EtOH), and water/methanol (MeOH) with volume ratio of 80/20 at room temperature were used as the first coagulation bath. This step was followed by immersion of the membrane into the second bath of distillated water for 1 day to remove the remaining solvent. The wet membranes were dried at room temperature for 1 day.

Several series of experiments were carried out, changing the following variables:

- Thickness of membrane (280, 300, 325, and 350 μm),
- PSF concentration in the casting solution (14, 18, and 22 wt %),
- type of solvent in the casting solution (DMF, NMP, DMAC, and THF),
- type of external nonsolvent (20% solution of MeOH, PrOH, EtOH, and IPA),
- immersion time in the first coagulation bath,
- temperature of second coagulation bath,
- type of nonsolvent in the casting solution. One of the possibilities to create a more open and interconnected pore structure is by addition of nonsolvent into the casting solution, we called it internal nonsolvent, and
- addition of additive into the casting solution.

Membrane morphology

The morphology of the prepared membrane was examined by a Philips scanning electron microscope model XL30. Membranes were first frozen in liquid nitrogen and fractured. After sputtering with gold, they were viewed with the microscope at 25 kV.

Flux and selectivity evaluation

In nonporous membranes, the transport mechanism for gas separation is often solution diffusion. A well-known permeation equation is:

$$J = [DS(P_1 - P_2)]/L \quad (1)$$

where J is the permeation flux, D is the diffusion coefficient, S is the solubility coefficient, L is the membrane thickness, and P_1 and P_2 are the pressures on the two sides of the membrane. The pressure difference is the driving force causing separation. DS is called permeation coefficient.

$$P = DS \tag{2}$$

If eq. (4) is arranged for P, the permeability per length (permeance) is obtained as follows:

$$P/L = J/[(P_1 - P_2)] \tag{3}$$

The overall capability of a membrane to separate a pair gas is characterized by an ideal permselectivity factor that is based on, "diffusivity" and "sorption":

$$\alpha = [D_A/D_B][S_A/S_B] \tag{4}$$

In our study, we measured gas permeance for membranes at room temperature. The reported values are the average of four measurements.

RESULTS AND DISCUSSIONS

Membrane morphology

The morphology of the membranes prepared via dual bath depends on the two types of phase separation processes. The membranes were formed by contacting a polymer solution with two successive nonsolvent baths. In the first bath delayed and in the second bath instantaneous phase, separation processes were developed. The diffusion process starts at the interface between casting film and nonsolvent in the first bath to produce a membrane with an asymmetric structure. The examples of the first bath compositions were IPA, PrOH, EtOH, and MeOH. In the second bath, mainly water, the polymer concentration in the sublayer or support is not significantly changed. This step provides an open and porous structure.[9]

Figure 2 represents the SEM images for two different systems. The first micrograph [Fig. 2(a)] shows the structure of the membrane immersed in water bath for 24 h without immersion into the second bath. No distinctive skin layer was formed. The cross section of a membrane consists of a long tear and finger-like pores extending to the bottom of the membrane. The oxygen permeance through the membrane was 45.3 $m^3/(m^2$ h bar) at 0.5 bar with no selectivity for separation of oxygen from nitrogen. This indicates that gas transport was predominantly determined by pore flow. The result demonstrates that the skin layer of the membrane prepared by wet phase inversion was highly defective. The reason for establishment of this structure may be

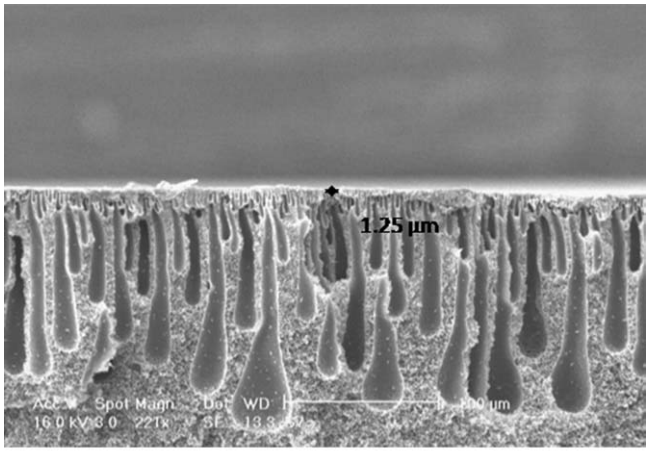

(a)

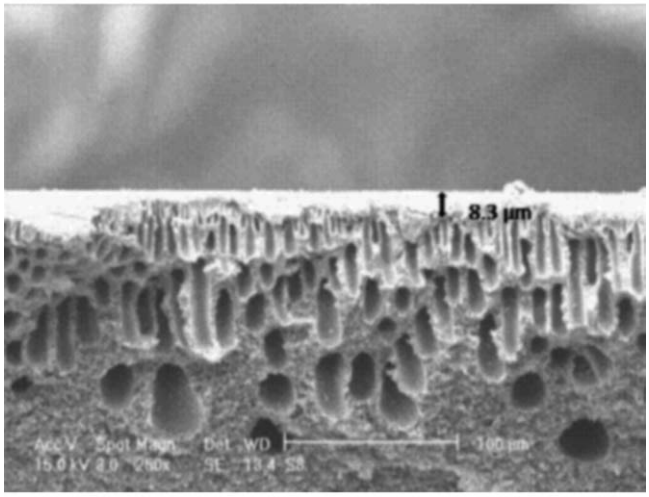

(b)

Figure 2 SEM micrographs of the membranes with different coagulation baths. (a) Distillated water bath for 24 h and (b) IPA as first coagulation bath for 80 s and distillated water as second coagulation bath for 24 h.

explained as follows. The liquid–liquid phase separation is instantaneous since the solvent (NMP) in the polymer solution is rapidly exchanged with water which is very polar.[9] Water is a highly polar nonsolvent with no interaction with NMP which is a polar solvent.

Figure 2(b) shows the SEM of the cross-sectional view of the membrane immersed in the second coagulation bath (distilled water) for 24 h after being immersed in the first IPA bath for 80 s. The first IPA bath was employed to obtain a concentrated layer of the polymer at the interface. The cross section of the membrane consists of spongy like structure and short finger like pores. The membrane skin layer is thick and dense, which would cause a further decline in oxygen flux. The reason for this phenomenon is the delayed liquid–liquid phase separation between NMP as solvent and IPA as nonsolvent. IPA as a low polar nonsolvent has interaction with NMP as a polar solvent. The oxygen permeance for

TABLE I
Oxygen Permeance as a Function of Different Casting Thicknesses

	Oxygen permeance (m^3/m^2 h bar)							
Pressure (bar) / Thickness (μm)	0.5 ± 0.1	1 ± 0.1	1.5 ± 0.1	2 ± 0.1	2.5 ± 0.1	3 ± 0.1	3.5 ± 0.1	4 ± 0.1
280	0	0.157 ± 0.004	0.328 ± 0.004	0.514 ± 0.004	0.566 ± 0.004	0.737 ± 0.004	0.740 ± 0.004	0.755 ± 0.004
300	0	0.126 ± 0.004	0.310 ± 0.004	0.492 ± 0.004	0.533 ± 0.004	0.686 ± 0.004	0.690 ± 0.004	0.745 ± 0.004
325	0	0.056 ± 0.004	0.168 ± 0.004	0.252 ± 0.004	0.312 ± 0.004	0.328 ± 0.004	0.330 ± 0.004	0.377 ± 0.004
350	0	0	0.049 ± 0.004	0.212 ± 0.004	0.226 ± 0.004	0.230 ± 0.004	0.300 ± 0.004	0.320 ± 0.004

PSF in NMP, first coagulation bath IPA for 80 s, second coagulation bath distillated water at 20°C.

this membrane was 0.049 $m^3/(m^2$ h bar) at 1.5 bar with 9.81 selectivity for separation of oxygen from nitrogen.

Influence of casting thickness

A series of membranes were prepared by wet casting of a 22 wt % PSF solution in NMP. The membranes were cast on glass plate with thicknesses of 280, 300, 325, and 350 μm. The membranes were immersed in the first coagulation bath of IPA immediately after casting. The wet film was maintained in the first bath for 80 s and moved to the second coagulation bath of distillated water at 20°C for 1 day. Demixing occurred during one day in the second bath.

Oxygen permeance as a function of casting thickness and different feed pressure for the prepared membrane is shown in Table I. By increasing the casting thickness, oxygen permeance was declined and selectivity was improved. This is due to an increment in the thickness of the skin layer. The arrows on Figure 3 clearly indicate the thicknesses of the formed skin layers on the surfaces of the membranes. The thicknesses of the established skin layers were 1.1 and 8.3 μm for the membranes with the casting thicknesses of 280 and 350 μm. The membrane with thicker skin layer provides higher resistance against passing gas leading to permeance diminishment. The proposed morphology is due to lower diffusion rate of nonsolvent to the thicker casting film. This leads to delayed liquid–liquid phase demixing.

Oxygen/nitrogen selectivity as a function of casting thickness and different feed pressure is presented in Figure 4. The selectivity was improved more than threefolds (3 vs. 10) by increasing the casting thickness from 280 to 350 μm. The selectivity enhancement may be explained on the basis of membrane structure. Figure 3 indicates the alteration of macro-voids to the shorter finger-like pores in the

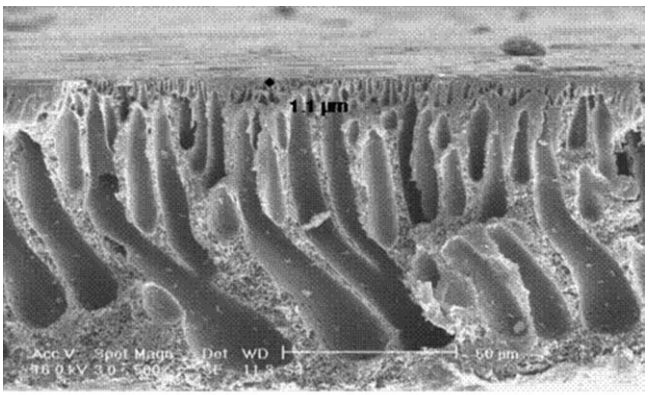

Figure 3 SEM micrographs of the membranes with different casting thicknesses: (a) 280 μm and (b) 350 μm.

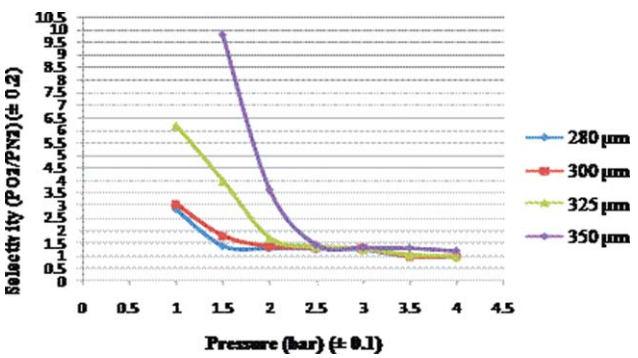

Figure 4 Oxygen selectivity as a function of different casting thicknesses. [Color figure can be viewed in the online issue, which is available at wileyonlinelibrary.com.]

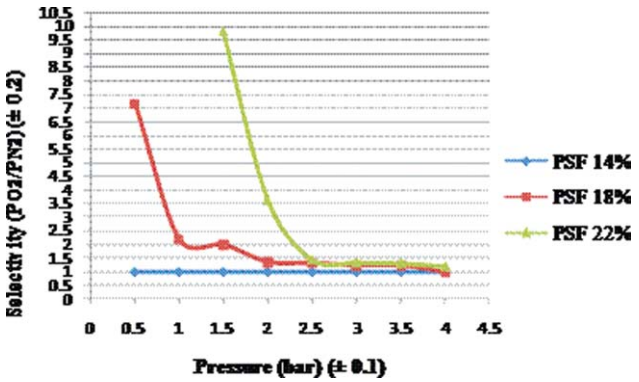

Figure 5 Oxygen selectivity as a function of different polymer concentrations (Casting solution, PSF in NMP; thickness of membrane, 350 μm; first coagulation bath, IPA for 80 s; second coagulation bath, distillated water 20°C). [Color figure can be viewed in the online issue, which is available at wileyonlinelibrary.com.]

upper part of the membrane by increasing the casting thickness. Moreover, the sponge-like structure is formed in the most parts of the membrane. This causes lower diffusion of nitrogen due to large size of nitrogen compared with oxygen molecules.

Influence of polymer concentration

To obtain a dense skin layer, the polymer concentration in the casting solution was further improved. Figure 5 shows the selectivity enhancement from one to around 10 by increasing the polymer concentration from 14 to 22%. The formation of a thick top layer and a sponge-like support with less macrovoid is evident (Fig. 6) at higher polymer concentration. The thicknesses of the skin layers were 2.4, 3.5, and 8.3 μm for polymer concentrations of 14, 18, and 22%, respectively. The establishment of this structure is due to higher resistance for exchange of solvent and nonsolvent for more concentrated polymer. This results in lower diffusion of gas molecules through the membrane. Further, reduction of macro-voids is desirable for improvement of the mechanical properties of the membranes.[10] However, some macrovoids are still present.

Influence of solvent type

Oxygen permeances of the membranes prepared from the casting solutions with different solvents are shown in Table II. The solvent type apparently affects the membrane permeance being lowest for DMF and highest for THF. A moderate permeance was found for the other two, i.e., NMP and DMAC solvents. This behavior is due to the solubility parameters (δsp) of various solvents. Many researchers have investigated the effect of different kinds of solvents on the membrane morphology.[11–16] The solubility parameters of solvents and nonsolvents are depicted in Table III.[17] The solubility parameter of four employed solvents followed the following order: DMF > NMP > DMAC > THF. Similar

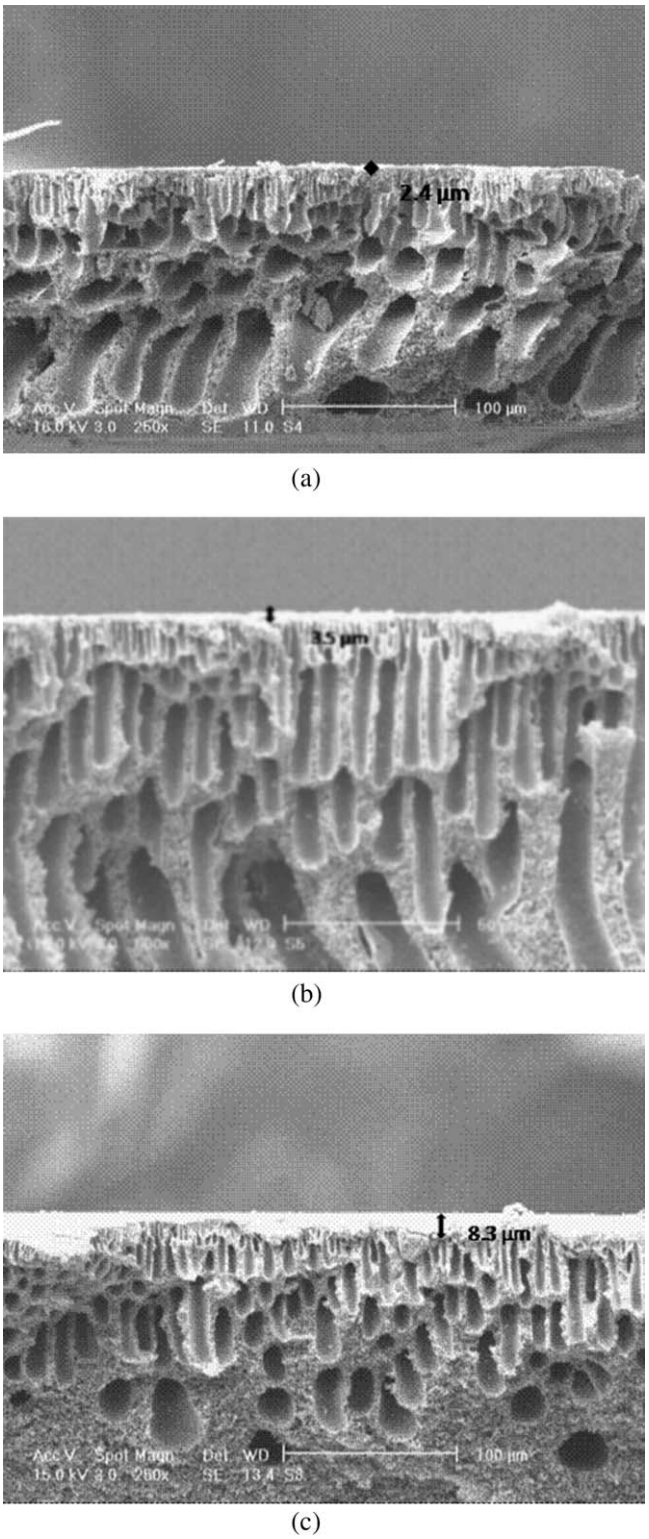

Figure 6 SEM micrographs of the membranes with different polymer concentrations: (a) 14 wt %, (b) 18 wt %, and (c) 22 wt %.

TABLE II
Oxygen Permeance as a Function of Different Solvents

	Oxygen permeance (m^3/m^2 h bar)							
Pressure (bar)	0.5 ± 0.1	1 ± 0.1	1.5 ± 0.1	2 ± 0.1	2.5 ± 0.1	3 ± 0.1	3.5 ± 0.1	4 ± 0.1
Solvent								
DMF	0	0	0	0	0	0	0.001 ± 0.004	0.015 ± 0.004
NMP	0	0	0.049 ± 0.004	0.210 ± 0.004	0.226 ± 0.004	0.230 ± 0.004	0.300 ± 0.004	0.320 ± 0.004
DMAC	0.100 ± 0.004	0.186 ± 0.004	0.270 ± 0.004	0.330 ± 0.004	0.335 ± 0.004	0.360 ± 0.004	0.381 ± 0.004	0.404 ± 0.004
THF	0.126 ± 0.004	0.226 ± 0.004	0.410 ± 0.004	0.420 ± 0.004	0.431 ± 0.004	0.444 ± 0.004	0.451 ± 0.004	0.472 ± 0.004

350 μm thickness, first coagulation bath IPA for 80 s, second coagulation bath distillated water at 20°C.

TABLE III
Solubility Parameters for Different Solvents and Nonsolvents[17]

Solvent and nonsolvent	Solubility parameter $(MJ/cm^3)^{1/2}$
DMF	24.8
NMP	22.9
DMAC	22.7
THF	18.6
IPA	23.8
PrOH	24.3
EtOH	26.0
MeOH	29.7
CHCl3	18.7
Distilled water	47.9

solubility parameters of solvent and nonsolvent result in a delay for leaving the solvent from the polymeric solution due to a strong interaction with nonsolvent.[18] In other words a delayed liquid–liquid phase demixing is developed. This produces a membrane with thicker skin layer and denser support. During the required time for introducing the nonsolvent to the film and solvent withdrawal, the polymer particles substitute the solvent leading to an enhancement in solid content and formation of a thick skin layer.

For determination of the nonsolvent bath solubility parameter, we may multiply nonsolvents solubility parameters by nonsolvents moles. The nonsolvent bath for this work was the mixture of distilled water and IPA with volume ratio of 80/20. Solubility parameter for this nonsolvent bath was 43.08 $(MJ/cm^3)^{1/2}$. The solubility parameter of THF as solvent has the maximum difference with nonsolvent solubility parameter, i.e., when THF is used as the solvent, instantaneous liquid–liquid phase demixing is developed. The solubility parameter of DMF has the minimum difference with nonsolvent solubility parameter. This causes delayed liquid–liquid phase demixing.

Influence of the external nonsolvent

A series of membranes were prepared by wet casting of a 22 wt % PSF in NMP using different alcohols in the first coagulation bath. By using IPA as the external nonsolvent, the oxygen permeance for the prepared membrane reached to a minimum. However, the oxygen permeance was higher for PrOH, EtOH, and MeOH as nonsolvents (Table IV). Figure 7 illustrates the oxygen selectivity for the membranes prepared from different external nonsolvents. The highest selectivity of 9.81 was obtained for IPA. This was gradually declined for PrOH and EtOH and reached to a minimum for MeOH.

At a constant nonsolvent concentration, the membrane morphology is strongly changed as a function of nonsolvent type. The membrane overall thickness was improved in the order of MeOH < EtOH < PrOH < IPA. Figure 8 shows the skin layer thicknesses as 2.2, 6.7, and 8.3 μm for membranes using MeOH, EtOH, and IPA as nonsolvent, respectively. These results are in good agreement with various studies on the effect of the coagulation medium

TABLE IV
Oxygen Permeance as a Function of Different Nonsolvents

	Oxygen permeance (m^3/m^2 h bar)							
Pressure (bar)	0.5 ± 0.1	1 ± 0.1	1.5 ± 0.1	2 ± 0.1	2.5 ± 0.1	3 ± 0.1	3.5 ± 0.1	4 ± 0.1
Nonsolvent								
IPA 20%	0	0	0.049 ± 0.004	0.210 ± 0.004	0.226 ± 0.004	0.230 ± 0.004	0.300 ± 0.004	0.320 ± 0.004
PrOH 20%	0.300 ± 0.004	0.348 ± 0.004	0.472 ± 0.004	0.472 ± 0.004	0.503 ± 0.004	0.521 ± 0.004	0.588 ± 0.004	0.629 ± 0.004
EtOH 20%	0.393 ± 0.004	0.435 ± 0.004	0.604 ± 0.004	0.629 ± 0.004	0.645 ± 0.004	0.686 ± 0.004	0.719 ± 0.004	0.745 ± 0.004
MeOH 20%	0.404 ± 0.004	0.526 ± 0.004	0.629 ± 0.004	0.659 ± 0.004	0.697 ± 0.004	0.795 ± 0.004	0.863 ± 0.004	1.130 ± 0.004

PSF in NMP, 350 μm thickness, second coagulation bath distillated water at 20°C.

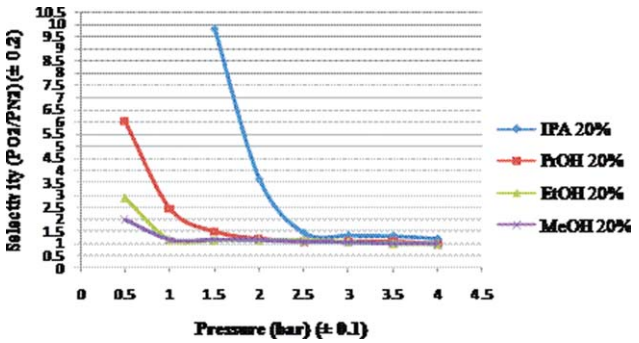

Figure 7 Oxygen selectivity as a function of different external nonsolvents. [Color figure can be viewed in the online issue, which is available at wileyonlinelibrary.com.]

and conditions on the morphology and gas separation properties of asymmetric membranes (e.g., Refs. 19–22). These studies indicate that in general, the top layer thickness of the membrane is improved with increasing molar volume of the external nonsolvent, due to the lower diffusion rate, which leads to delayed liquid–liquid phase demixing. Figure 8 indicates that the overall membrane thickness was improved and the void volume (porosity) was declined from MeOH to IPA.

Influence of second bath temperature

The oxygen permeance and selectivity are depicted in Figure 9 as a function of different temperatures of second coagulation bath. The immersion times in the first coagulation bath of IPA were 30 and 80 s. With increasing the temperature in the range of 20–40°C, the oxygen permeance through the membrane was improved and the oxygen selectivity was declined. The reason behind this behavior is the rate of demixing between solvent and nonsolvent. By temperature enhancement in the second coagulation bath, the rate of demixing between solvent and nonsolvent is improved. This causes instantaneous liquid–liquid phase demixing leading to the formation of thin skin layer with high permeance and low selectivity. This morphology is confirmed by SEM micrograph. Figure 10 represents the membrane structure immersed in the first coagulation bath of IPA for 80 s and in the second coagulation bath of distillated water at 40°C. The membrane possesses a thin skin layer with a porous support, whereas the membrane that was immersed in the first coagulation bath of IPA for 80 s and the second coagulation bath of distillated water at 20°C showed a very distinctive skin layer [Fig. 8(c)].

Influence of internal nonsolvent

One of the techniques for preparing membrane with more open structure is the addition of nonsolvent to the casting solution.[23] Lai et al.[20] found that alcohols with greater molecular weights are most efficient for the reduction of the skin layer thickness for polymeric membranes. Accordingly while IPA was used as the external coagulant, different nonsolvents with concentration of 3 wt % were added to the casting solution.

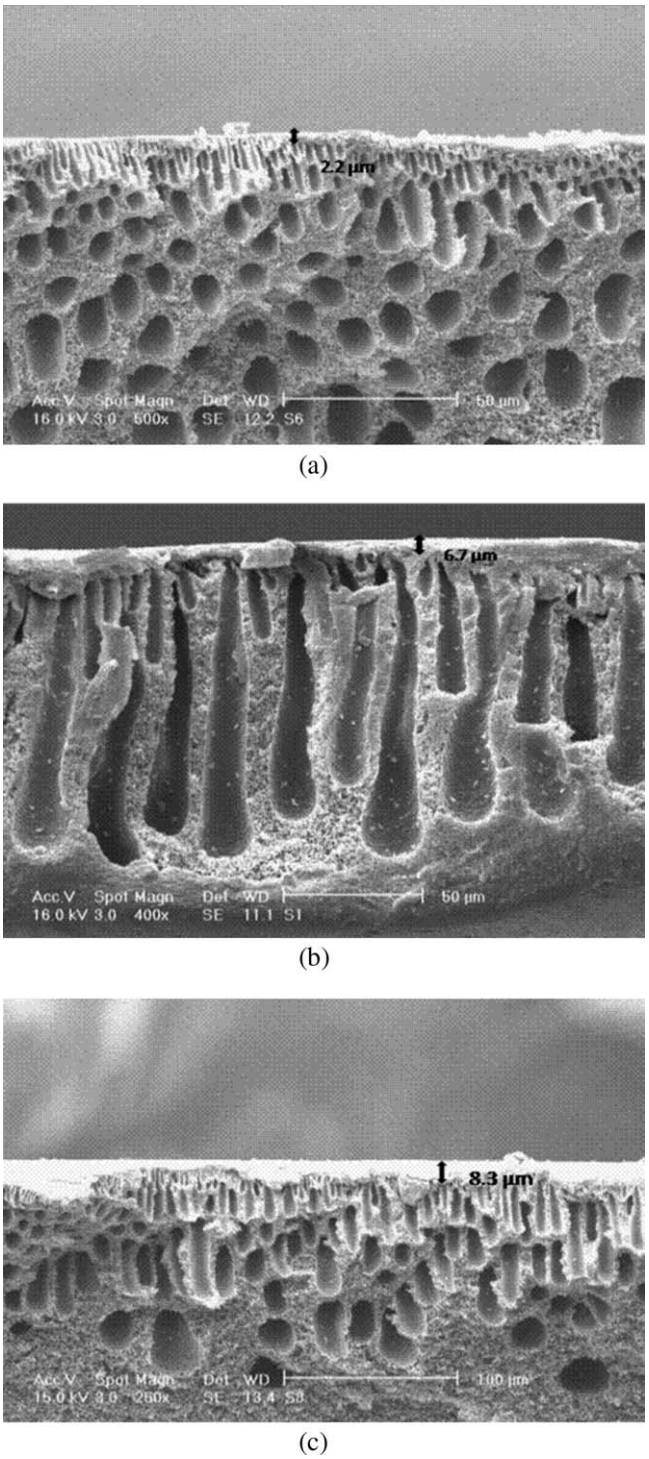

(a) (b) (c)

Figure 8 SEM micrographs of the membranes with different external nonsolvents. (a) MeOH, (b) EtOH, and (c) IPA.

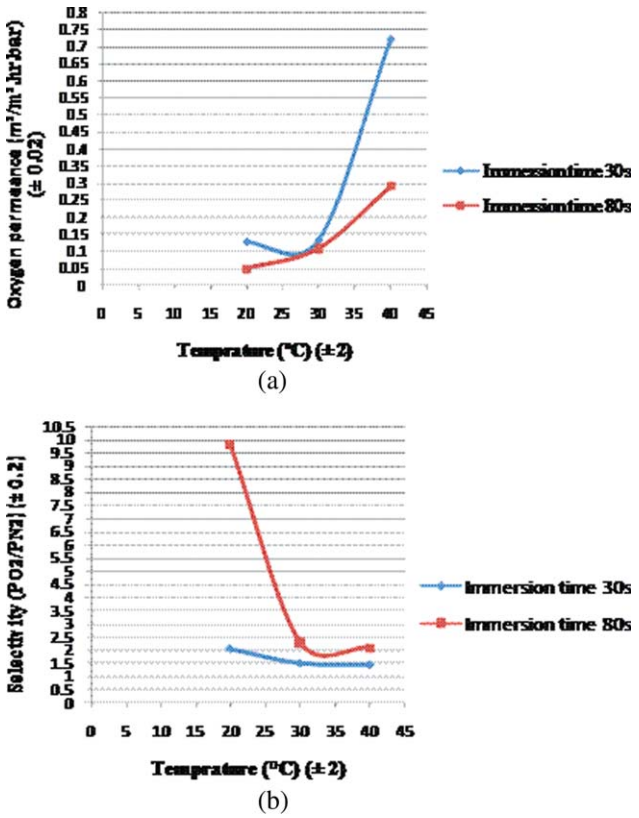

Figure 9 Effect of the second coagulation bath temperature on oxygen permeance (a) and oxygen selectivity (b) (casting solution, PSF in NMP; thickness of membrane, 350 μm; first coagulation bath, IPA; second coagulation bath, distillated water). [Color figure can be viewed in the online issue, which is available at wileyonlinelibrary.com.]

In comparison with the membrane without internal nonsolvent [Fig. 11(a)], MeOH created an open structure. This reduced the thickness of the skin layer from 8.3 to 6.8 μm [Fig. 11(b)]. Further reduction in skin layer thickness (2.3 μm) was observed by introducing BuOH to the casting solution [Fig. 11(c)]. For the current case, the membrane turned to a macro-porous media due to the formation of a void support layer. The greater molecular weight of BuOH is the primary difference among the alcohols and the main reason for various structures.

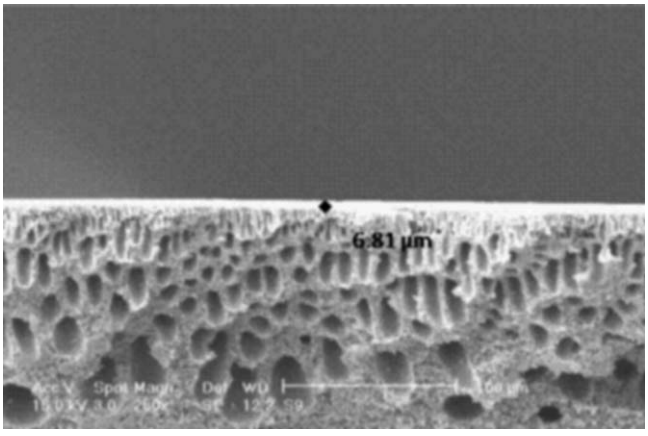

Figure 10 SEM micrograph of the membrane immersed in IPA for 80 s and in distillated water at 40°C.

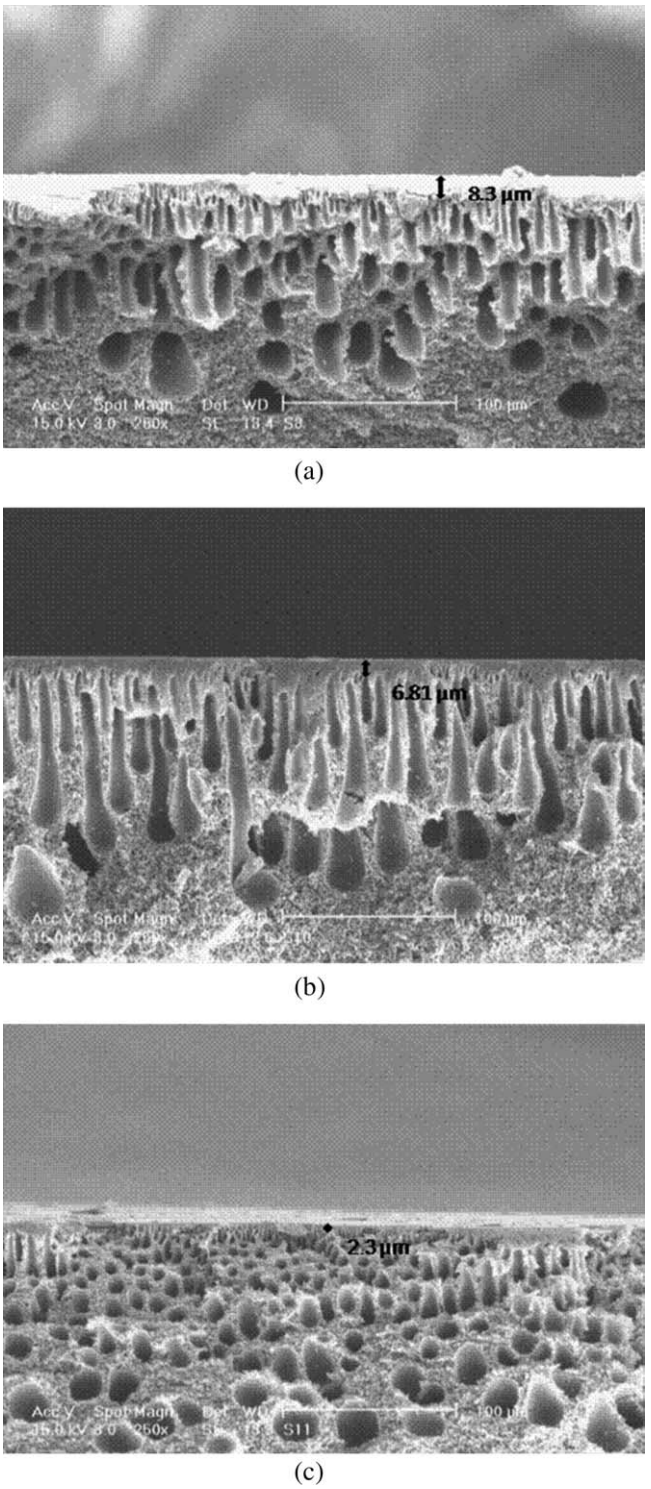

Figure 11 SEM micrographs of the membranes with different internal nonsolvents: (a) Without internal nonsolvent, (b) MeOH, and (c) BuOH.

TABLE V
Oxygen Permeance as a Function of Different Internal Nonsolvents

	Oxygen permeance (m^3/m^2 h bar)							
Pressure (bar)	0.5 ± 0.1	1 ± 0.1	1.5 ± 0.1	2 ± 0.1	2.5 ± 0.1	3 ± 0.1	3.5 ± 0.1	4 ± 0.1
Internal nonsolvent								
Not added	0	0	0.05 ± 0.01	0.21 ± 0.01	0.22 ± 0.01	0.23 ± 0.01	0.30 ± 0.01	0.32 ± 0.01
MeOH	0.70 ± 0.01	0.90 ± 0.01	1.16 ± 0.01	1.41 ± 0.01	1.51 ± 0.01	1.89 ± 0.01	2.00 ± 0.01	2.30 ± 0.01
EtOH	1.19 ± 0.01	1.30 ± 0.01	1.37 ± 0.01	1.45 ± 0.01	1.65 ± 0.01	1.96 ± 0.01	2.30 ± 0.01	2.50 ± 0.01
IPA	1.23 ± 0.01	1.40 ± 0.01	1.58 ± 0.01	1.70 ± 0.01	2.00 ± 0.01	2.40 ± 0.01	2.90 ± 0.01	3.20 ± 0.01
BuOH	1.33 ± 0.01	1.49 ± 0.01	1.60 ± 0.01	1.77 ± 0.01	2.10 ± 0.01	2.60 ± 0.01	3.20 ± 0.01	3.50 ± 0.01

PSF in NMP, 350 μm thickness, first coagulation bath IPA for 80 s, second coagulation bath distillated water at 20°C.

By using BuOH as the internal nonsolvent, the oxygen permeance for the prepared membrane reached to a maximum (Table V). However, the oxygen permeance was lower for IPA, EtOH, and MeOH as the internal nonsolvents. Previous study[24] indicates that BuOH is an efficient pore former. Figure 12 illustrates the oxygen selectivity for the membranes prepared from different internal nonsolvents. The highest selectivity of 9.81 was obtained for casting solution without addition of internal nonsolvent. This was gradually declined for MeOH (around 6), EtOH, and IPA (both around 3) as the internal nonsolvents and reached to a minimum (around 2) for BuOH. This is consistent with the high open structure of the membrane obtained by addition of BuOH.

Influence of PVP as additive

PVP with different concentrations (nil up to 7 wt %) was added to the casting solution containing 22 wt % PSF to investigate the effect of PVP concentration on membrane morphology and performance. After addition of a low quantity (3 wt %) of PVP in the casting solution, the oxygen permeance for the prepared membrane reached to a maximum of 0.9 m^3/m^2 h bar [Fig. 13(a)]. However, the oxygen permeance was lower for further addition of PVP in the casting solution (0.4 m^3/m^2 h bar for 7 wt %). The highest selectivity of 9.81 was obtained for casting solution without addition of PVP. This was declined and reached to a minimum of 2 for 3 wt % PVP. However, the oxygen selectivity was improved for further addition of PVP in the casting solution and reached to 5 for introducing 7 wt % of PVP [Fig. 13(b)].

Figure 14 shows the cross-sectional images of the membranes prepared from PSF (22 wt %) and 0, 3, and 7 wt % PVP. The addition of 3 wt % PVP in the

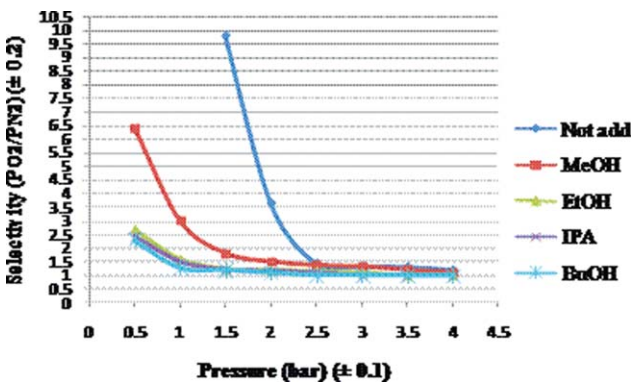

Figure 12 Oxygen selectivity as a function of different internal nonsolvents. [Color figure can be viewed in the online issue, which is available at wileyonlinelibrary.com.]

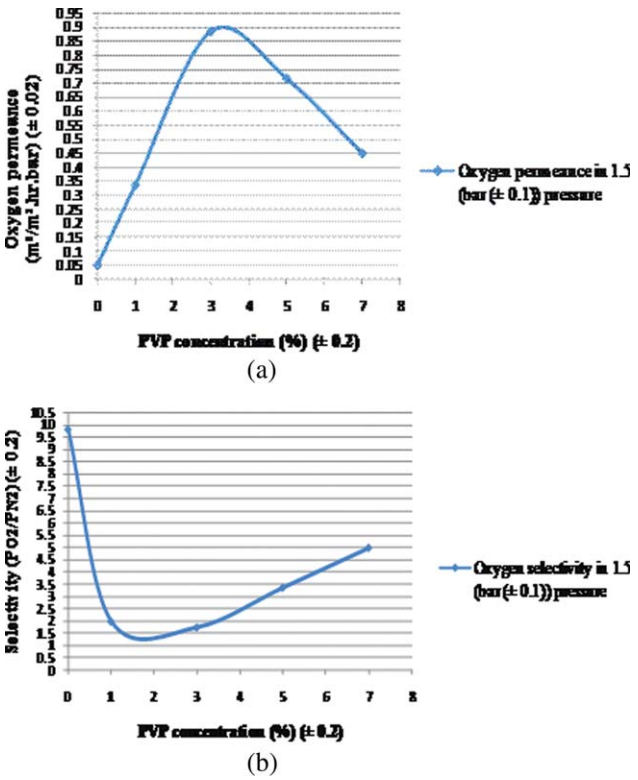

Figure 13 Effect of the PVP concentration on oxygen permeance (a) and oxygen selectivity (b) (casting solution, PSF in NMP; thickness of membrane, 350 μm; first coagulation bath, IPA for 80 s; second coagulation bath, distillated water 20°C). [Color figure can be viewed in the online issue, which is available at wileyonlinelibrary.com.]

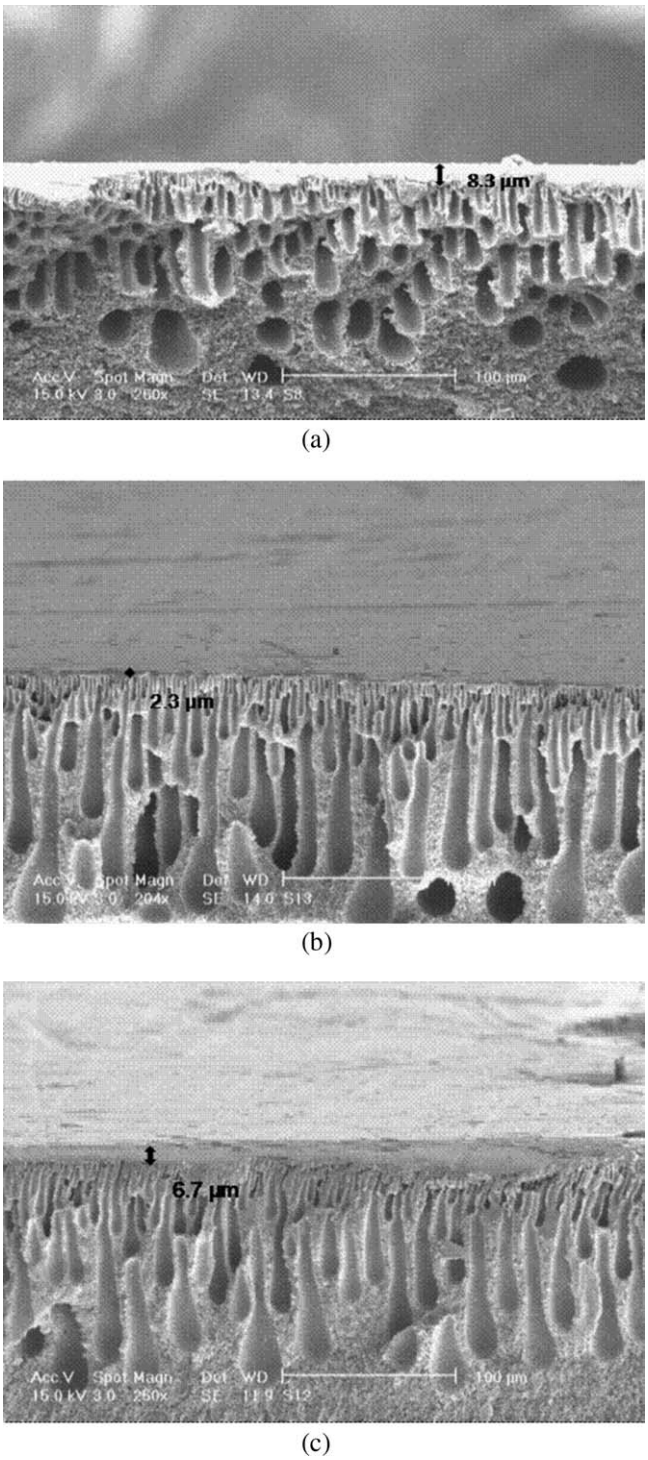

(a)

(b)

(c)

Figure 14 SEM micrographs of the membranes with different concentrations of PVP: (a) 0 wt %, (b) 3 wt %, and (c) 7 wt %.

casting solution changed the membrane morphology from thick dense top layer (8.3 μm) and non-finger-like pores [Fig. 14(a)] to a thin top layer (2.3 μm) with fully developed finger-like pores [Fig. 14(b)]. When the PVP concentration was improved in the casting solution, the membrane structure was converted into the original state (without PVP) and gradually a membrane with thicker top layer (6.7 μm) and denser support layer was formed [Fig. 14(c)]. It is known that the morphology of membrane depends on the content of PVP.[25] In the current research, we found that the top-layer thickness is improved and the porosity of sublayer is reduced by more addition of PVP.

The changes in the membrane morphology can be attributed to and explained by the interactions between components in the casting solution and phase inversion kinetics.[25] When the concentration of PVP in the casting solution is 3 wt %, PVP functions as a pore former leading to a membrane with higher porosity in sublayer.[26] However, when the concentration of PVP in the casting solution rises to 7 wt %, the interaction between PVP and NMP as solvent is improved and delayed liquid–liquid phase separation is developed. This results in membrane with distinctive skin layer.

CONCLUSIONS

A wet/wet phase separation process in combination with two series of nonsolvent baths was used to prepare ultrathin and defect free asymmetric PSF membranes for gas separations. With the increment of the casting thickness and polymer concentration, the flux of the prepared membranes was reduced and the oxygen selectivity was improved. The solvent type apparently affects the membrane permeance being lowest for DMF and highest for THF. This behavior is due to the solubility parameters of various solvents. By using IPA as the external nonsolvent, the oxygen permeance reached to a minimum. However, the oxygen permeance was higher for PrOH, EtOH, and MeOH as nonsolvent. The thickness of the top layer is improved with increasing molar volume of the external nonsolvent due to low diffusion rate, which leads to delayed liquid–liquid demixing. With increasing the temperature of the second coagulation bath in the range of 20–40°C, the oxygen permeance of the membrane was improved and the oxygen selectivity was declined. By temperature enhancement in the second coagulation bath, the rate of demixing between solvent and nonsolvent is improved. This causes instantaneous liquid–liquid phase demixing leading to the formation of thin skin layer with high permeance and low selectivity. Addition of internal nonsolvent to the casting solution resulted in a decline in the thickness of the active layer and an improvement in the oxygen permeance. Finally, the oxygen permeance was enhanced and reached to a maximum by addition of small quantity (3 wt %) of PVP. This was reduced with further addition of PVP in the casting solution.

References

1. Koros, W. J.; Mahajan, R. J Membr Sci 2001, 181, 141.
2. Van Thof, J. A.; Reuvers, A. J.; Boom, R. M.; Rolevink, H. H. M.; Smolders, C. A. J Membr Sci 1992, 70, 17.
3. Pinnau, I.; Koros, W. J. J Appl Polym Sci 1991, 43, 1491.
4. Pesek, S. C.; Koros, W. J. J Membr Sci 1993, 81, 71.
5. Kapantaidakis, G. C.; Kaldis, S. P.; Dabou, X. S.; Sakellaropoulos, G. P. J Membr Sci 1996, 110, 239.
6. Van Baal, H.; Goosy, M. Plastics for Electronics; Kluwer Academic Publishers: Dordrecht, 1999; Vol. 51.
7. Pinnau, I.; Freeman, B. D. Am Chem Soc 1999, 744, 1.
8. Han, M. J.; Bhattacharyya, D. Chem Eng Commun 1993, 128, 197.
9. Lee, W. J.; Kim, D. S.; Kim, J. H. Korean J Chem Eng 2000, 17, 143.
10. Radovanovic, P.; Thiel, S. W.; Hwang, S. T. J Membr Sci 1992, 65, 231.
11. Yang, J. M.; Hsiue, G. H.; Chen, H. L. Polym Eng Sci 1996, 36, 425.
12. Li, Z.; Ren, J.; Fane, A. G.; Li, D. F.; Wong, D. S. J Membr Sci 2006, 279, 601.
13. Wu, L.; Sun, J.; Wang, Q. J Membr Sci 2006, 285, 290.
14. Kneifel, K.; Peinemann, K. V.; Paul, D. J Membr Sci 2001, 192, 217.
15. Chun, K. Y.; Jang, S. H.; Kim, H. S.; Kim, Y. W. J Membr Sci 2000, 169, 197.
16. Miyano, T.; Matsuura, T.; Sourirajan, S. Chem Eng Commun 1990, 95, 11.
17. Bottino, A.; Roda G. C.; Capannelli, G. J Membr Sci 1991, 57, 1.
18. Brandrup, J.; Immergent, E. H. Polymer Handbook, 2nd ed.; Wiley: New York, 1975.
19. Mulder, M. H. V.; Oude Hendrikman, J.; Wijmans, J. G.; Smolders, C. A. J Appl Polym Sci 1985, 30, 2805.
20. Lai, J. Y.; Liu, M. J.; Lee, K. R. J Membr Sci 1994, 86, 103.
21. Radovanovic, P.; Thiel, S. W.; Hwang, S. T. J Membr Sci 1992, 65, 231.
22. Lin, F. C.; Wang, D. M.; Lai, J. Y. J Membr Sci 1996, 110, 25.
23. Jansen, J. C.; Buonomenna, M. G.; Figoli, A.; Drioli, E. J Membr Sci 2006, 272, 188.
24. Jansen, J. C.; Macchione, M.; Drioli, E. J Membr Sci 2005, 255, 167.
25. Rahimpour, A.; Madaeni, S. S. J Membr Sci 2007, 305, 299.
26. Wu, L.; Sun, J.; Wang, Q. J Membr Sci 2006, 285, 290.